COPY NO. 3
RM No. E7F13

NACA

RESEARCH MEMORANDUM

INVESTIGATION OF SHOCK DIFFUSERS AT MACH NUMBER 1.85

III - MULTIPLE-SHOCK AND CURVED-CONTOUR PROJECTING CONES

By W. E. Moeckel and J. F. Connors

Flight Propulsion Research Laboratory
Cleveland, Ohio

NATIONAL ADVISORY COMMITTEE
FOR AERONAUTICS

WASHINGTON

August 13, 1947

NATIONAL ADVISORY COMMITTEE FOR AERONAUTICS

RESEARCH MEMORANDUM

INVESTIGATION OF SHOCK DIFFUSERS AT MACH NUMBER 1.85

III - MULTIPLE-SHOCK AND CURVED-CONTOUR PROJECTING CONES

By W. E. Moeckel and J. F. Connors

SUMMARY

Total-pressure recoveries were obtained with four cone-inlet combinations at Mach number 1.85. The configurations investigated were as follows: a cone designed to produce three oblique shocks ahead of the diffuser inlet in combination with a straight and a curved inlet section; a cone generated by a parabolic arc, also in combination with a curved and a straight inlet section; a cone-inlet combination designed by the method of characteristics to produce an isentropic entrance flow at an angle of attack of 0°; and a 30° single-shock cone in combination with a perforated inlet section. The effect of angle of attack was also investigated for the isentropic configuration.

Each of these configurations yielded total-pressure recoveries greater than those reported in references 1 and 2. A maximum total-pressure recovery of 0.967 was attained with the isentropic configuration. For the triple-shock, parabolic-arc, and perforated-inlet configurations, the maximum recoveries were 0.954, 0.950, and 0.954, respectively. At an angle of attack of 5°, the maximum total-pressure recovery obtained with the isentropic configuration was reduced to 0.922.

INTRODUCTION

An investigation of shock diffusers at a Mach number of 1.85 has been conducted in the Cleveland 18- by 18-inch supersonic tunnel. Results obtained with a shock diffuser having a single oblique shock ahead of the diffuser inlet are presented in reference 1. In reference 2 the results obtained with cones designed to produce two oblique shocks ahead of the inlet are reported. With the single-shock cones, a maximum total-pressure recovery of 0.922 was obtained, whereas with the double-shock cones the maximum recovery was 0.945.

Because the deceleration of the supersonic airstream to sonic velocity can be accomplished more efficiently with a large number of weak shocks than with one or two relatively intense ones, even higher total-pressure recoveries than those reported in references 1 and 2 can theoretically be obtained by increasing the number of breaks in the projecting-cone contour and reducing the flow deflection produced by each break. The ideal configuration is attained when the deceleration is produced so gradually that no shocks are formed in the air entering the diffuser. The ideal contour of the projecting cone is therefore a smoothly curved surface that produces an infinite number of infinitesimal compression waves. From supersonic-flow theory, however, it is known that such a series of infinitesimal compression waves tends to converge and form an envelope shock through which the entire compression takes place (reference 3). Hence the contour required for isentropic compression is not arbitrary, but must be so designed that the compression waves converge outside the entering stream tube. A contour having this property may be designed by the method of characteristics (reference 4). Such a contour should decelerate the supersonic stream with no total-pressure loss if frictionless flow is assumed.

The problem of decelerating a supersonic stream to sonic velocity with negligible total-pressure loss thus offers no theoretical difficulties when the flow is decelerated ahead of the inlet. The external deceleration, however, may be accompanied by increased pressures over the external surfaces of the diffuser relative to the pressures that would result if the deceleration were accomplished internally (as, for example, with a convergent-channel diffuser). Hence a higher drag may be expected for shock diffusers employing external compression relative to that obtained with convergent-channel diffusers. This additional drag must at least partly cancel the higher thrusts possible with the higher total-pressure recoveries.

The total-pressure recovery hitherto obtainable with a convergent-channel diffuser has been limited by the starting requirement that the contraction ratio may not exceed the value required to accelerate the subsonic velocity behind a normal shock at free-stream Mach number to sonic velocity at the throat (reference 5). A greater contraction ratio would result in choking at the throat and would prevent the normal shock from entering the inlet consequently, the supersonic stream could be brought to subsonic velocities only by passing through a relatively intense normal shock.

This limit to the contraction ratio allowable with a convergent-channel diffuser may be eliminated by a method proposed

in reference 6. The method consists of allowing some of the air mass to bleed through perforations drilled in the convergent channel, whereas normally the excess air would have to spill around the entrance lip. Choking at the throat is thereby avoided. By this method, the normal shock could be brought to the throat of the diffuser and stabilized there, even when the inlet contraction ratio was large enough to reduce the free-stream flow to sonic velocity (reference 6). Hence the total-pressure recoveries obtainable with a convergent-channel diffuser are now theoretically as great as those obtainable with external compression. Accompanying the higher total-pressure recovery possible with the convergent perforated inlet is an additional drag due to the mass-flow loss through the perforations. During operation this mass-flow loss is much smaller than during the starting process because the pressure difference across the holes after the normal shock has passed them is much less than when the flow is subsonic.

The mass-flow loss through the holes can be reduced by using the perforated inlet with a shock diffuser. Reference 6 shows that the excess mass flow which must be bled through the perforations during the starting process decreases, as the inlet Mach number decreases. The presence of a projecting central body therefore offers a means of minimizing the number of perforations required and consequently the mass-flow loss during operation. The compression waves from the projecting body may be intercepted by the inlet to avoid high external pressures and the inlet Mach number may be reduced to unity by internal contraction. The use of a perforated inlet with a properly designed shock diffuser may thus provide a means of attaining supersonic diffusion with negligible total-pressure loss together with a minimum external drag and mass-flow loss.

These improved types of supersonic inlet were investigated with the following four configurations: A, a cone designed to produce three oblique shocks ahead of the diffuser inlet; B, a cone generated by a parabolic arc; C, a cone-inlet combination designed by the method of characteristics; and D, a 30° single-shock cone in combination with a perforated inlet section. For each of these configurations, the variation of total-pressure recovery with outlet area was determined. The variation of total-pressure recovery with tip projection was determined for configurations A, B, and C. Configuration D was investigated only at the tip projection for which the oblique shock just entered the diffuser inlet. For configuration C, the effect of angle of attack was also investigated.

SYMBOLS

The following symbols are used in this report:

A_0 free-stream area of flow that enters diffuser

A_2 minimum flow area of diffuser

A_4 outlet area of simulated combustion chamber

A_e inlet area of diffuser with central body in place

A_i inlet area of diffuser with central body removed

P_0 free-stream total pressure

P_4 total pressure in simulated combustion chamber

L tip projection, inches

X axial coordinate

Y radial coordinate

DESCRIPTION OF EXPERIMENTAL APPARATUS

The investigation was conducted in the Cleveland 18- by 18-inch supersonic tunnel operating at Mach number 1.85. The tunnel was calibrated by measurements of the angles of oblique shocks from cones and of the total pressures behind normal shocks. The absolute values of total pressure and Mach number in the test section determined by these measurements are accurate within about 2 percent. The relative measured total-pressure recoveries reported, however, are accurate within about 0.5 percent.

Sketches of the four configurations investigated are shown in figure 1. Configuration A is a triple-shock cone with included angles of 30° at the tip, 50° after the first break, and 60° after the second break. Approximate calculations based on the flow near the cone surface indicated that this combination of included angles would yield an optimum total-pressure recovery. For configuration B, a parabolic arc was passed between the tip half-angle (10°) and the maximum half-angle (30°). The length

[redacted]

of the contour was arbitrarily set equal to that of the triple-shock cone. The inlet sections used with configurations A and B were those used in references 1 and 2.

Configuration C was designed by the method of characteristics to decelerate the flow to sonic velocity with no total-pressure loss. An expanded plot of the contour coordinates, together with the location of a few of the characteristics, is shown in figure 2. At the tip of the cone, the contour angle was arbitrarily set at 6°. The total-pressure ratio across the oblique shock produced by this cone angle is very near 1.00. A region beyond the assumed location of the diffuser inlet was chosen for the convergence of the compression waves. The characteristics from this region were then computed toward the X-axis. Streamlines were drawn from the cone tip to point a and from d to e. The Mach number at points a and e were found to be 1.15 and 1.29, respectively. Point e was chosen for the location of the entrance lip and the process of turning the flow parallel to the axis was started at this point. The only requirement for the contour e to f was that the compressions starting at this contour should not intersect before reaching the central body. The cone contour was extended linearly from a to b, where it intersected the first characteristic arriving from e. The curve b-c was then drawn in to cancel the compression waves arriving from e-f. The total-flow contraction ratio A_0/A_2 is very close to the isentropic contraction ratio for a free-stream Mach number M_0 of 1.85. The ratio of the inlet area (e-b, fig. 2) to the minimum area A_2 is 1.025, which is close to the isentropic contraction ratio from a Mach number of 1.15 to unity. From one-dimensional-flow relations, this contraction ratio is small enough to allow a normal shock occurring at Mach numbers greater than 1.19 to enter the diffuser. The average inlet Mach number according to the calculations is 1.22

Configuration D (fig. 1) was used to test the principle of the perforated inlet (reference 6) with a shock diffuser. The 30° single-shock cone investigated in reference 1 was used in combination with a straight inlet section into which holes were drilled. The number of holes required was experimentally determined.

The diffuser body and simulated combustion chamber were those used in references 1 and 2 (fig. 3). The outlet area of the diffuser was again varied by means of the conical damper located at the outlet of the simulated combustion chamber and total and static pressures at the simulated combustion chamber were measured with a pitot-static rake located as shown in figure 3(a). The cone support and the inlets used with configurations A, B, and D are shown in figures 3(b) to 3(e). For configuration D, the

[redacted]

straight inlet of figure 3(c) was perforated with a number of holes sufficient to allow the normal and oblique shocks to enter the diffuser inlet. By trial it was found that the shocks entered the diffuser inlet when 50 holes of 0.161-inch diameter and 15 holes of 3/32-inch diameter had been drilled ahead of the throat section. The ratio of hole area to throat area was then 0.45.

For configuration C, a new cone support was constructed that was similar to the one shown in figure 3(b) except that the maximum diameter was 1.455 inches instead of 1.290 inches.

RESULTS AND DISCUSSION

Typical inlet-flow patterns. - Schlieren photographs of the inlet flow with each of the four configurations are shown in figure 4. Figures 4(a) and 4(b) show the flow patterns obtained for configuration A with the straight and the curved inlets, respectively, for the tip projection and outlet area for which maximum total-pressure recovery was obtained. As with the double-shock cones (reference 2), two oblique shocks arise near the first break in the cone contour, one slightly ahead of the break and one slightly beyond it. This effect is attributed to a bridging of the break by the boundary layer. At the second break in the cone contour, a fourth oblique shock arises. With the straight inlet (fig. 4(a)), this shock merges indistinguishably with the bow wave that stands ahead of the diffuser inlet. With the curved inlet (fig. 4(b)), the bow wave is somewhat closer to the inlet and a portion of the fourth oblique shock was distinguishable in the original negative.

The flow over the parabolic-arc cone (configuration B, fig. 1) is shown in figures 4(c) and 4(d) for the conditions giving the maximum total-pressure recovery with the straight and curved inlets, respectively. The compression waves from the cone surface can be seen to converge ahead of the inlet. The resulting envelope shock is of appreciable intensity and, as might be expected, the maximum total-pressure recoveries are slightly below those obtained with configuration A, where each of the shocks is very weak. The vertical lines from the bow wave to the cone surface are projections of the bow wave, whereas the wave itself curves toward the interior of the diffuser.

The flow over the isentropic cone (configuration C) for two outlet areas at an angle of attack of 0° and for the optimum outlet area at an angle of attack of 5° is shown in figures 4(e), 4(f),

and 4(g). A number of weak compression waves may be seen that tend to converge beyond the inlet, although not so far beyond the inlet as the calculations (fig. 2) assumed. The existence of visible compression waves and their tendency to converge somewhat nearer the cone surface than predicted may be attributed to boundary-layer effects or small machining flaws. In figure 4(g), which shows the configuration at an angle of attack of 5°, the compression ripples from the lower surface are seen to converge into a discernible envelope shock. The bow wave stands ahead of the inlet in each of these three photographs.

An effort was made to bring the normal shock into the diffuser in this configuration by perforating the inlet, but the total-pressure recovery dropped as the number of perforations was increased while the normal shock remained ahead of the inlet. This result indicates that for reasons of stability, the reduction of a supersonic stream to subsonic velocity may be impossible without the occurrence of at least a very weak shock discontinuity. Because the normal shock remained ahead of the inlet, the curvature of the inlet (fig. 2) was not critical in this case and served only to force a smooth deflection of the subsonic entrance flow. For the condition giving the best recovery (fig. 4(f)), the normal shock originates approximately at point a of figure 2.

The flow pattern for the 30° single-shock cone with perforated inlet is shown in figure 4(h). Because the external-flow pattern remained the same as the outlet area was varied, schlieren photographs were taken only for the conditions indicated in the figure. The oblique shock, as well as the normal shock, passes inside the inlet, and the flow, which in the preceding photographs spilled around the entrance lip, is here entering the diffuser. The mass flow through the perforations produces the series of weak oblique shock waves originating on the outer surface of the inlet section. (Only a few of the perforations are visible in the schlieren photograph, fig. 4(h).) The maximum total-pressure recovery obtained with this configuration was as great as that obtained with configuration A (the triple-shock cone).

Variation of total-pressure recovery with outlet area. - The theoretical variation of total-pressure recovery with outlet area is discussed in references 1 and 2. For configurations A and B (figs. 5(a) to 5(d)), the variation of total-pressure recovery with outlet-inlet area ratio is presented for three tip projections for each of the two inlets used. The term "supercritical" in these figures refers to the values of A_4 for which the mass flow remains constant as A_4 is varied. The term "subcritical" refers to the values of A_4 for which variations in A_4 affect the mass flow

[redacted]

through the diffuser. The tip projections for which data are presented are optimum, 1/16 inch less than optimum, and 1/16 inch greater than optimum. Similar data are plotted in figure 5(e) for configuration C. The peaks of the curves for this configuration are broader than those obtained with the other three cones. For configuration D, data were obtained for only the tip projection at which the oblique shock from the tip passed inside the inlet (fig. 5(f)). The results obtained for this configuration with the oblique shock outside and with an unperforated inlet are presented in reference 1.

A comparison of the maximum total-pressure recoveries obtained with configurations A, B, and C for various tip projections is presented in figure 6. The maximum total-pressure recovery obtained with configuration A was 0.954 with the curved inlet and 0.945 with the straight inlet. The maximum theoretical total-pressure recovery for this configuration, based on the shock angles at the cone surface, is about 0.985, or about 3 percent higher than the experimental value obtained with the curved inlet. In reference 2 the maximum experimental recovery (0.945) was also found to be about 3 percent below the theoretical value.

The optimum experimental tip projection for the triple-shock cone (fig. 6(a)) was that for which the four oblique shocks passed just outside the entrance lip. For the straight inlet, no internal contraction existed at optimum tip projection ($A_e/A_2 = 1.00$), whereas for the curved inlet an internal expansion existed ($A_e/A_2 = 0.753$). Because the entrance flow was subsonic (figs. 4(a) and 4(b)), the curved inlet, which produces a smoother entrance flow, yielded a higher total-pressure recovery than the straight inlet. These results also agree with those obtained with double-shock cones (reference 2).

For the parabolic-arc cone (fig. 6(b)), approximately equal maximum recoveries were obtained with the straight and curved inlets (0.950 and 0.948, respectively). These values are intermediate between the maximums attained with double-shock and triple-shock cones.

The cone designed to produce an isentropic entrance flow (configuration C, fig. 6(c)) yielded the highest total-pressure recovery attained during the investigation. This value of 0.967, as with the double-shock and triple-shock cones, is about 3 percent less than the maximum theoretical value of 1.00. It is therefore reasonable to assume that about 3 percent of the total-pressure loss was due to the subsonic portion of the diffuser and that configuration C was in fact operating with almost no total-pressure loss at an angle of attack of 0°. At an angle of attack of 5°, the maximum recovery dropped to

0.922 (fig. 7). With the single-shock and the double-shock cones, the maximum recoveries at angle of attack of 5° were 0.908 and 0.899, respectively (references 1 and 2).

Configuration D (30° cone with perforated inlet, fig. 5(d)) produced a maximum recovery of 0.954, which is equal to the maximum obtained with the triple-shock cone. Without the perforations, the maximum recovery attained with this configuration was 0.879 (reference 1). Hence a gain of over 8 percent in maximum total-pressure recovery was obtained by the use of perforations to increase the maximum allowable internal contraction ratio. The total contraction ratio A_1/A_2 for this configuration was 1.52, which is slightly greater than the contraction required to decelerate the free stream to sonic velocity.

For the configurations reported, the distribution of static and total pressures across the diffuser outlet was similar to the distributions obtained with single-shock and double-shock cones. Plots of this distribution are therefore omitted.

SUMMARY OF RESULTS

An investigation of four shock-diffuser inlet configurations to determine the total-pressure ratios obtainable at a Mach number of 1.85 gave the following results:

1. A cone designed to produce three oblique shocks ahead of the inlet yielded a maximum total-pressure recovery of 0.954 when used in combination with a curved inlet section. Four oblique shocks were found to arise from the cone surface, two of them near the first break in the cone contour.

2. A cone generated by a parabolic arc, with a tip half-angle of 10°, yielded a total-pressure recovery of 0.950. The compression waves from the parabolic contour converged to an envelope shock ahead of the diffuser inlet.

3. A cone-inlet combination designed by the method of characteristics to decelerate the flow to sonic velocity with no total-pressure loss gave a maximum total-pressure recovery of 0.937 at 0° angle of attack. Nearly all the total-pressure loss may be attributed to the subsonic portion of the diffuser. At an angle of attack of 5°, the maximum recovery was reduced to 0.922. The flow over the cone surface was similar to the computed flow field except that the convergence of the compression waves took place slightly closer to the cone surface than calculations indicated and several

compression waves were visible in the flow field. Both of these effects may be attributed to boundary-layer build-up or small machining flaws.

4. A 30° single-shock cone in combination with an inlet that was perforated to allow entry of the normal and oblique shocks yielded a maximum total-pressure recovery of 0.954.

Flight Propulsion Research Laboratory,
National Advisory Committee for Aeronautics,
Cleveland, Ohio.

REFERENCES

1. Moeckel, W. E., Connors, J. F., and Schroeder, A. H.: Investigation of Shock Diffusers at Mach Number 1.85. I - Projecting Single-Shock Cones. NACA RM No. E6K27, 1947.

2. Moeckel, W. E., Connors, J. F., and Schroeder, A. H.: Investigation of Shock Diffusers at Mach Number 1.85. II - Projecting Double-Shock Cones. NACA RM No. E6L13, 1947.

3. Anon.: Supersonic Flow and Shock Waves. A Manual on the Mathematical Theory of Non-Linear Wave Motion. AMP Rep. 38.2R, AMG-NYU No. 62, New York Univ., Appl. Math. Group, NDRC, Appl. Math. Panel, Aug. 1944.

4. Ferri, Antonio: Application of the Method of Characteristics of Supersonic Rotational Flow. NACA TN No. 1135, 1946.

5. Kantrowitz, Arthur, and Donaldson, Coleman duP.: Preliminary Investigation of Supersonic Diffusers. NACA ACR No. L5D20, 1945.

6. Evvard, John C., and Blakey, John W.: The Use of Perforated Inlets for Efficient Supersonic Diffusion. NACA RM No. E7C26, 1947.

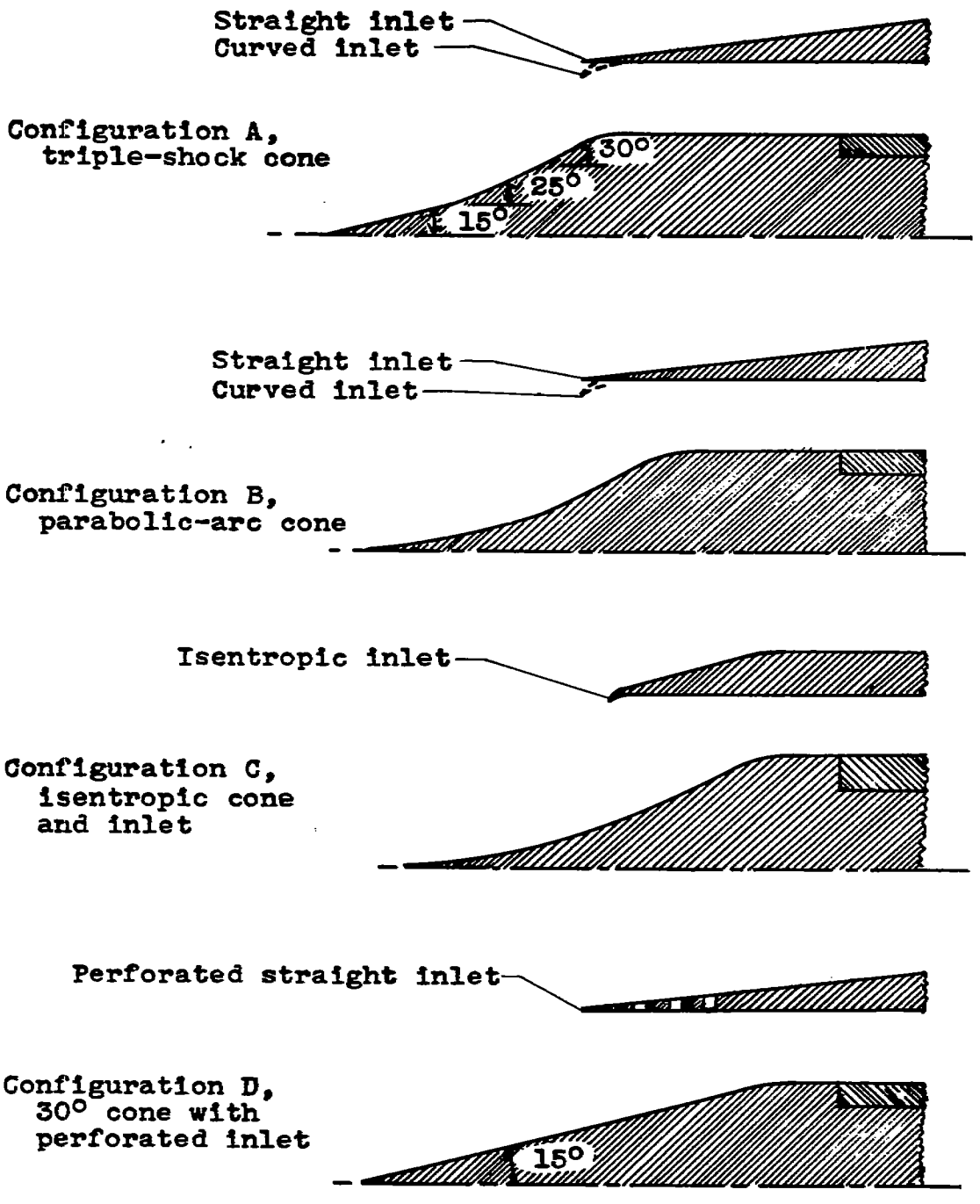

Figure 1.- Sketches of configurations investigated showing relative locations of cones and inlets at minimum tip projection.

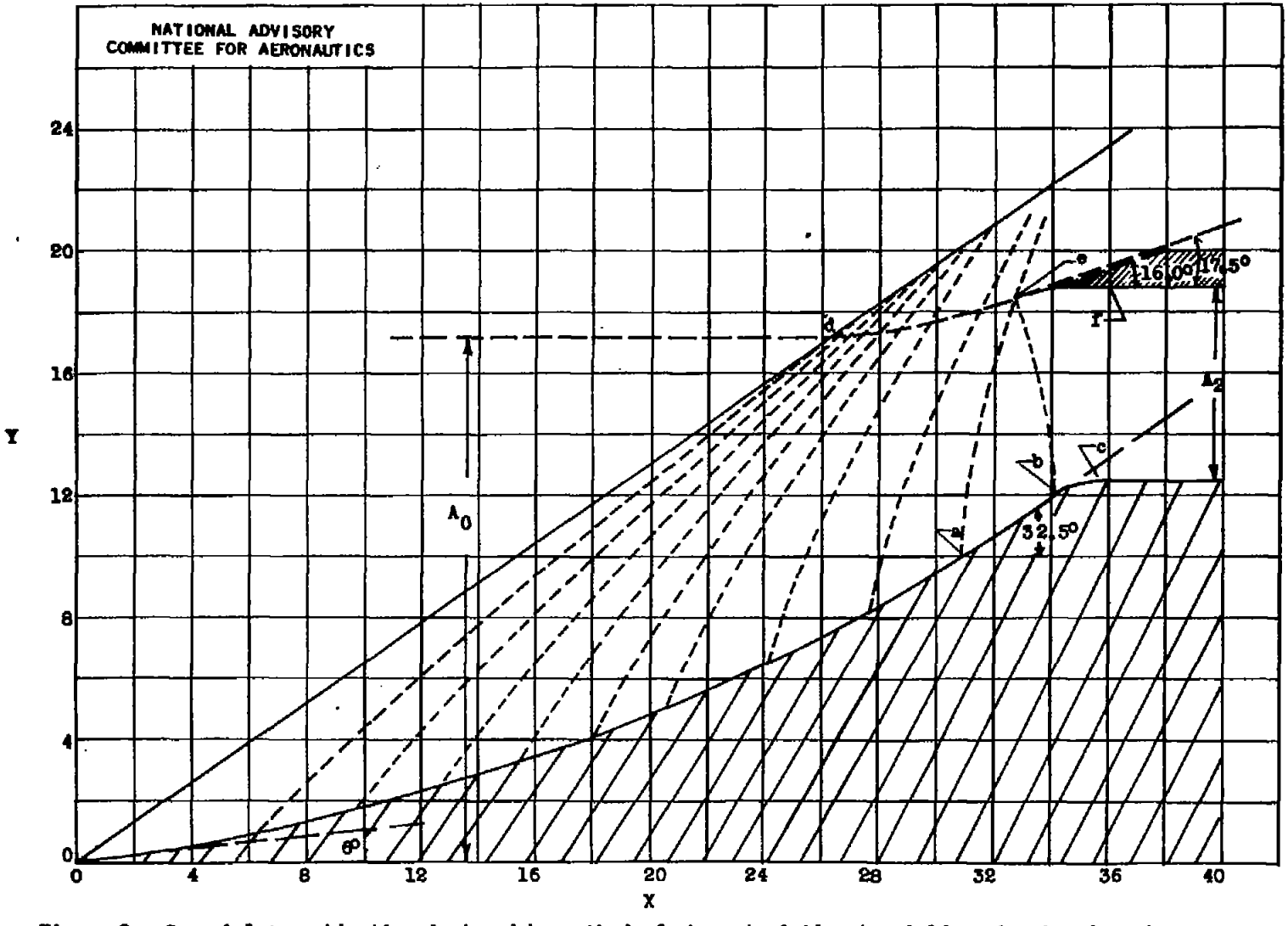

Figure 2.- Cone-inlet combination designed by method of characteristics to yield an isentropic entrance flow for $M_0 = 1.85$. (Arbitrary coordinate units.)

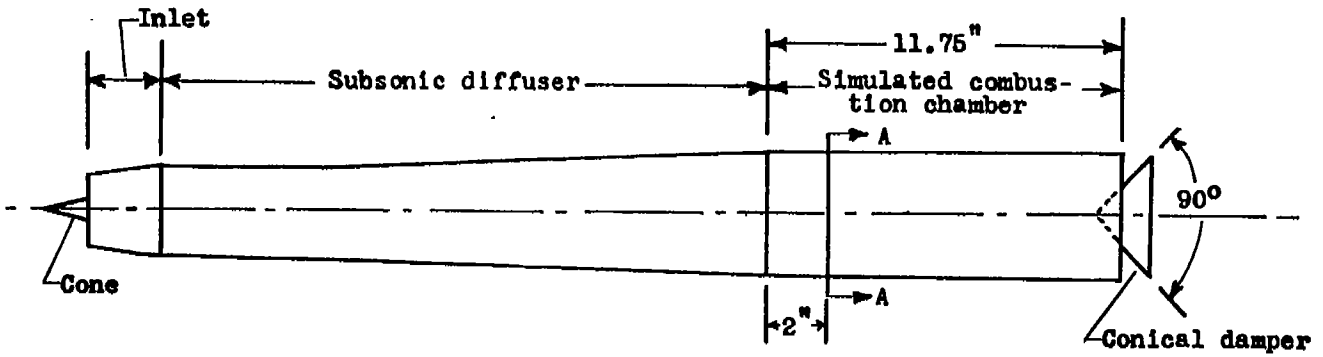

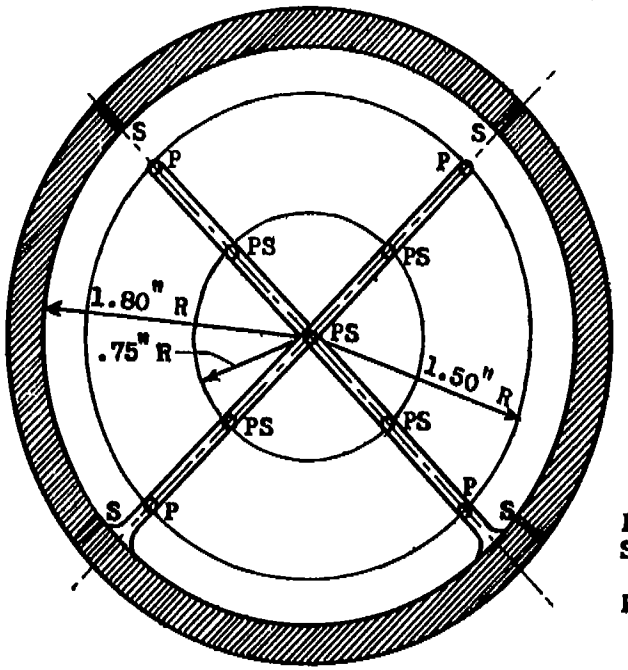

NATIONAL ADVISORY COMMITTEE FOR AERONAUTICS

P Pitot tube
S Static-pressure orifice
PS Pitot-static tube

Section A-A

(a) Schematic drawing of diffuser and simulated combustion chamber showing pressure instrumentation.

Figure 3. - Experimental model.

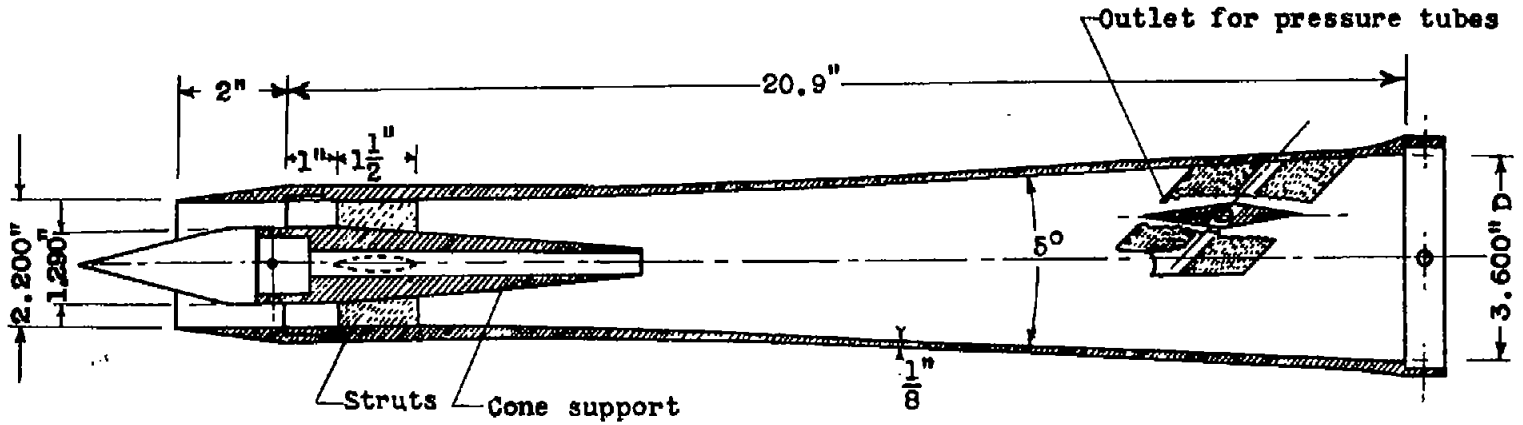

(b) Diffuser body and cone support.

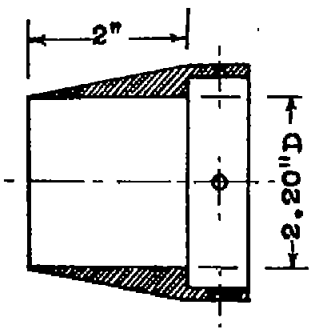

(c) Straight inlet.

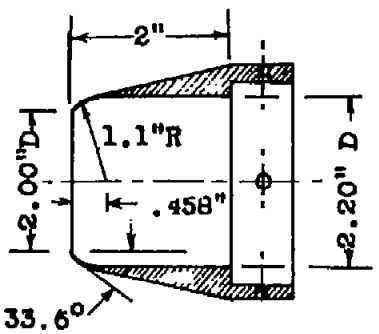

(d) Curved inlet.

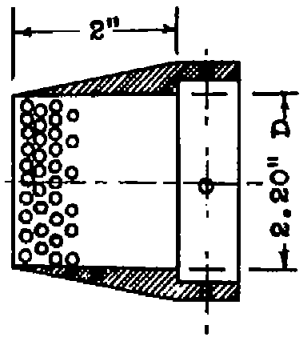

(e) Perforated straight inlet.

Figure 3.- Concluded. Experimental model.

NATIONAL ADVISORY
COMMITTEE FOR AERONAUTICS

(a) Configuration A; straight inlet; L, 1.69 inches; A_4/A_i, 0.526; P_4/P_0, 0.945; angle of attack, 0°.

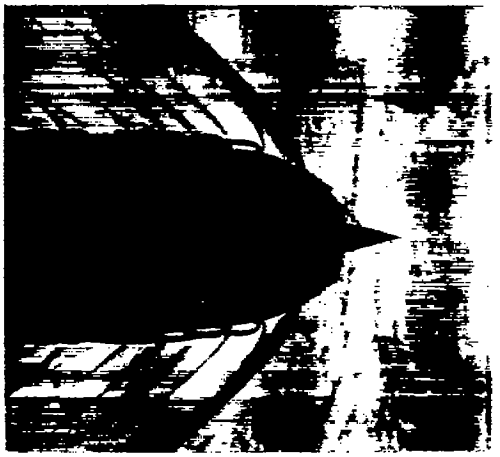

(b) Configuration A; curved inlet; L, 1.50 inches; A_4/A_i, 0.665; P_4/P_0, 0.954; angle of attack, 0°.

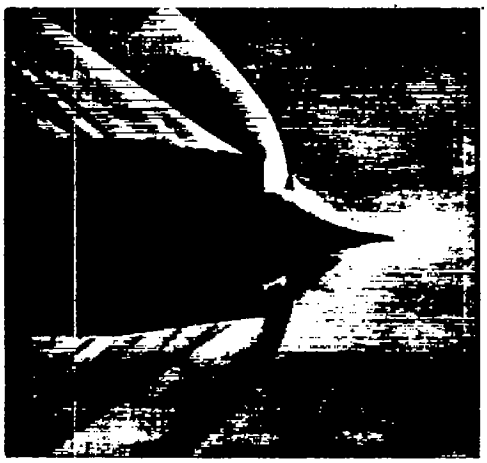

(c) Configuration B; straight inlet; L, 1.875 inches; A_4/A_i, 0.520; P_4/P_0, 0.950; angle of attack, 0°.

NACA
C-18861
5-27-47

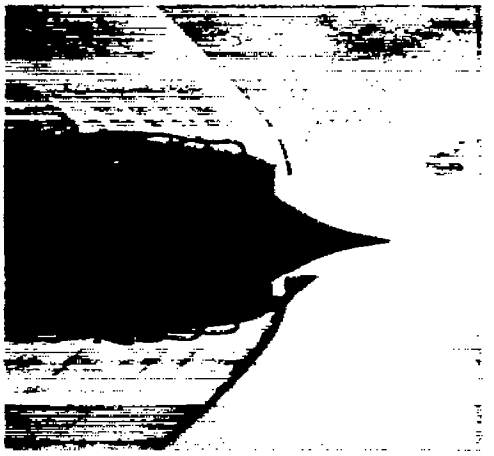

(d) Configuration B; curved inlet; L, 1.69 inches; A_4/A_i, 0.562; P_4/P_0, 0.948; angle of attack, 0°.

Figure 4. - Schlieren photographs of typical flow patterns.

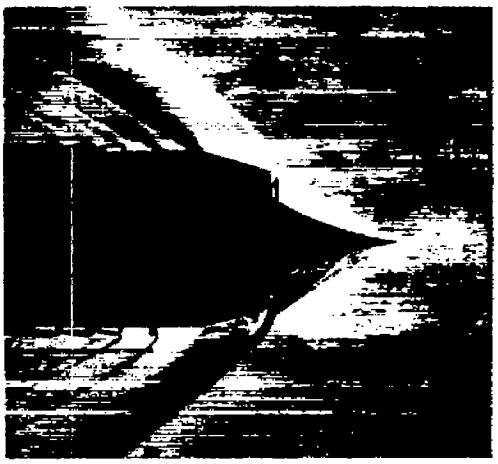

(e) Configuration C; isentropic inlet; L, 1.97 inches; A_4/A_i, 1.157; P_4/P_0, 0.529; angle of attack, 0°.

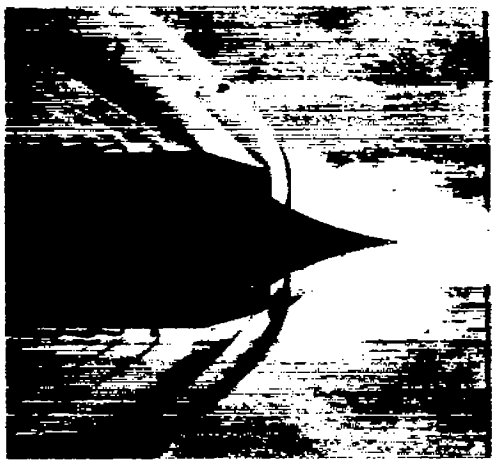

(f) Configuration C; isentropic inlet; L, 1.97 inches; A_4/A_i, 0.551; P_4/P_0, 0.964; angle of attack, 0°.

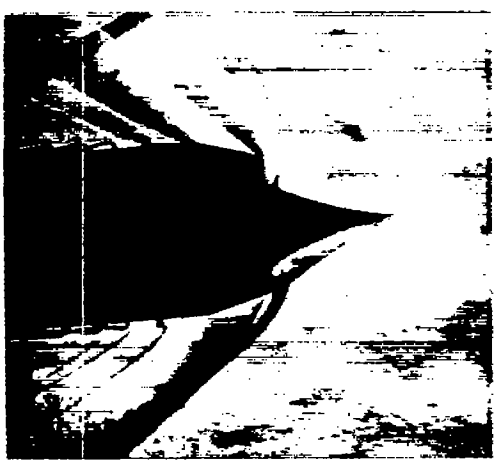

(g) Configuration C; isentropic inlet; L, 1.97 inches; A_4/A_i, 0.687; P_4/P_0, 0.918; angle of attack, 5°.

NACA
C-18862
5-27-47

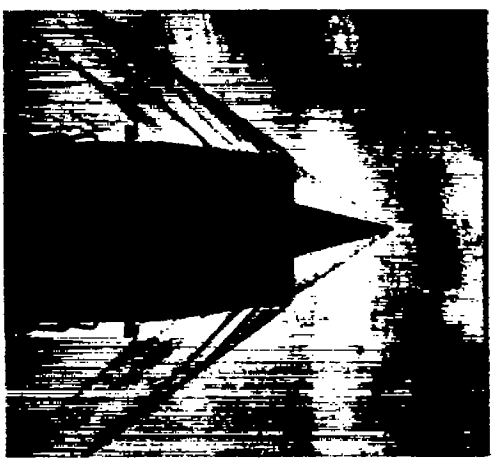

(h) Configuration D; perforated straight inlet; L, 1.49 inches; A_4/A_i, 1.075; P_4/P_0, 0.668; angle of attack, 0°.

Figure 4. - Concluded. Schlieren photographs of typical flow patterns.

[redacted]

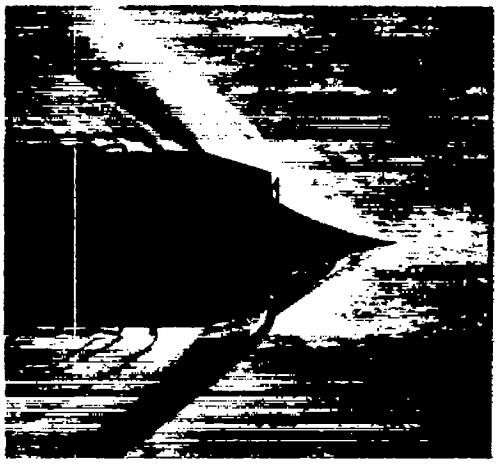

(e) Configuration C; isentropic inlet; L, 1.97 inches; A_4/A_i, 1.157; P_4/P_0, 0.529; angle of attack, 0°.

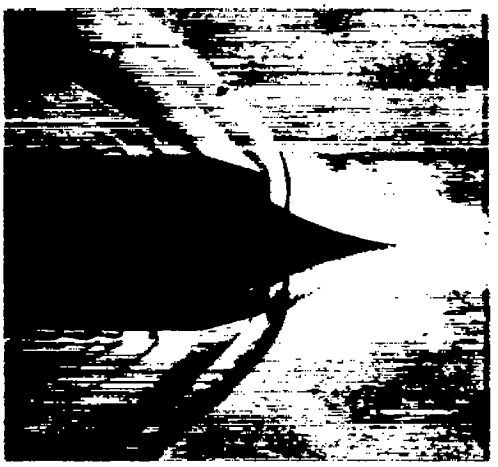

(f) Configuration C; isentropic inlet; L, 1.97 inches; A_4/A_i, 0.551; P_4/P_0, 0.964; angle of attack, 0°.

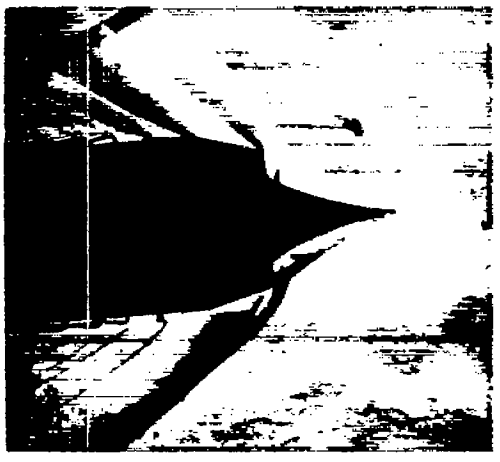

(g) Configuration C; isentropic inlet; L, 1.97 inches; A_4/A_i, 0.687; P_4/P_0, 0.918; angle of attack, 5°.

NACA
C-18862
5-27-47

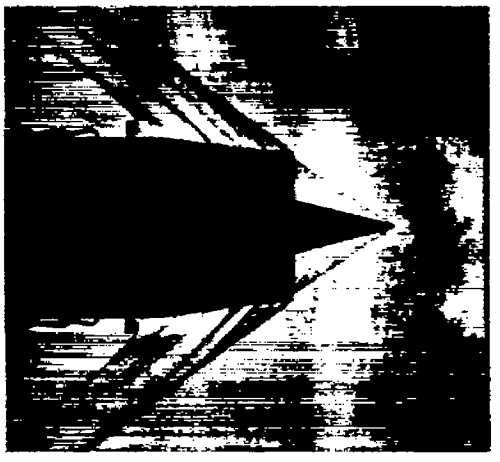

(h) Configuration D; perforated straight inlet; L, 1.49 inches; A_4/A_i, 1.075; P_4/P_0, 0.668; angle of attack, 0°.

Figure 4. - Concluded. Schlieren photographs of typical flow patterns.

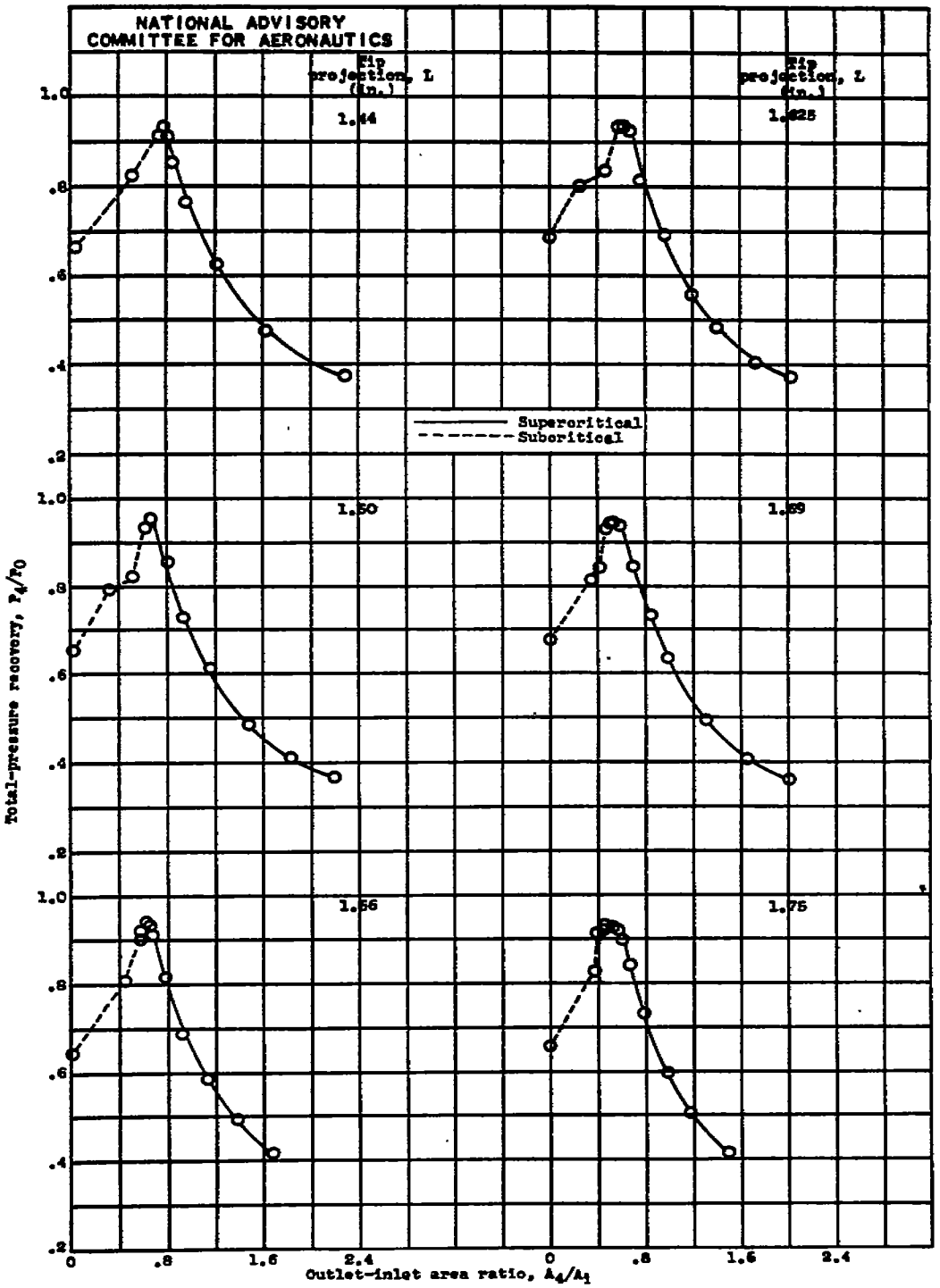

(a) Configuration A, triple-shock cone, curved inlet.

(b) Configuration A, triple-shock cone, straight inlet.

Figure 5.- Variation of total-pressure recovery with outlet-inlet area ratio at angle of attack of 0°.

[redacted]

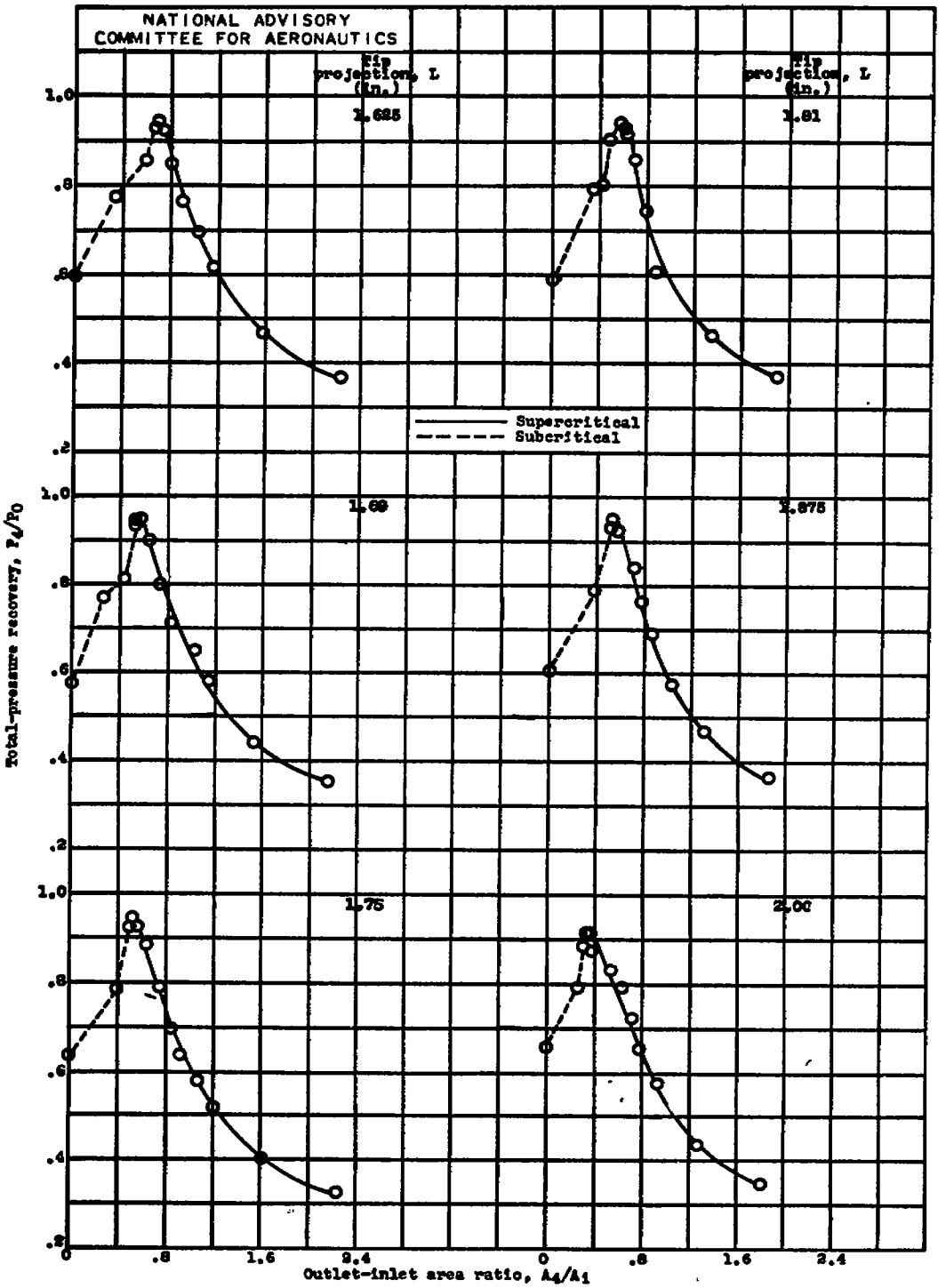

(c) Configuration B, parabolic-arc cone, curved inlet.

(d) Configuration B, parabolic-arc cone, straight inlet.

Figure 5.- Continued. Variation of total-pressure recovery with outlet-inlet area ratio at angle of attack of 0°.

[redacted]

-782

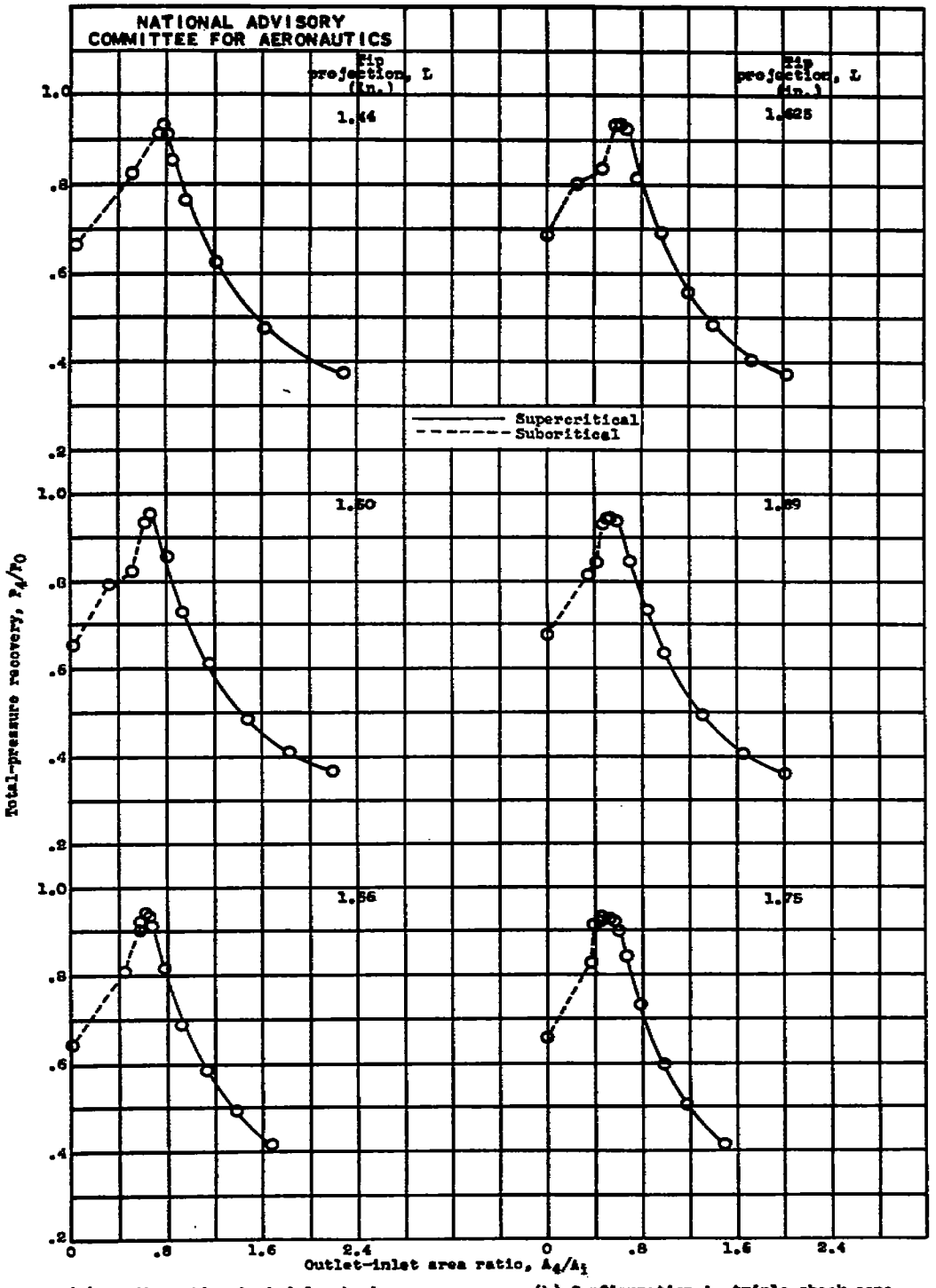

(a) Configuration A, triple-shock cone, curved inlet.

(b) Configuration A, triple-shock cone, straight inlet.

Figure 5.- Variation of total-pressure recovery with outlet-inlet area ratio at angle of attack of 0°.

[redacted]

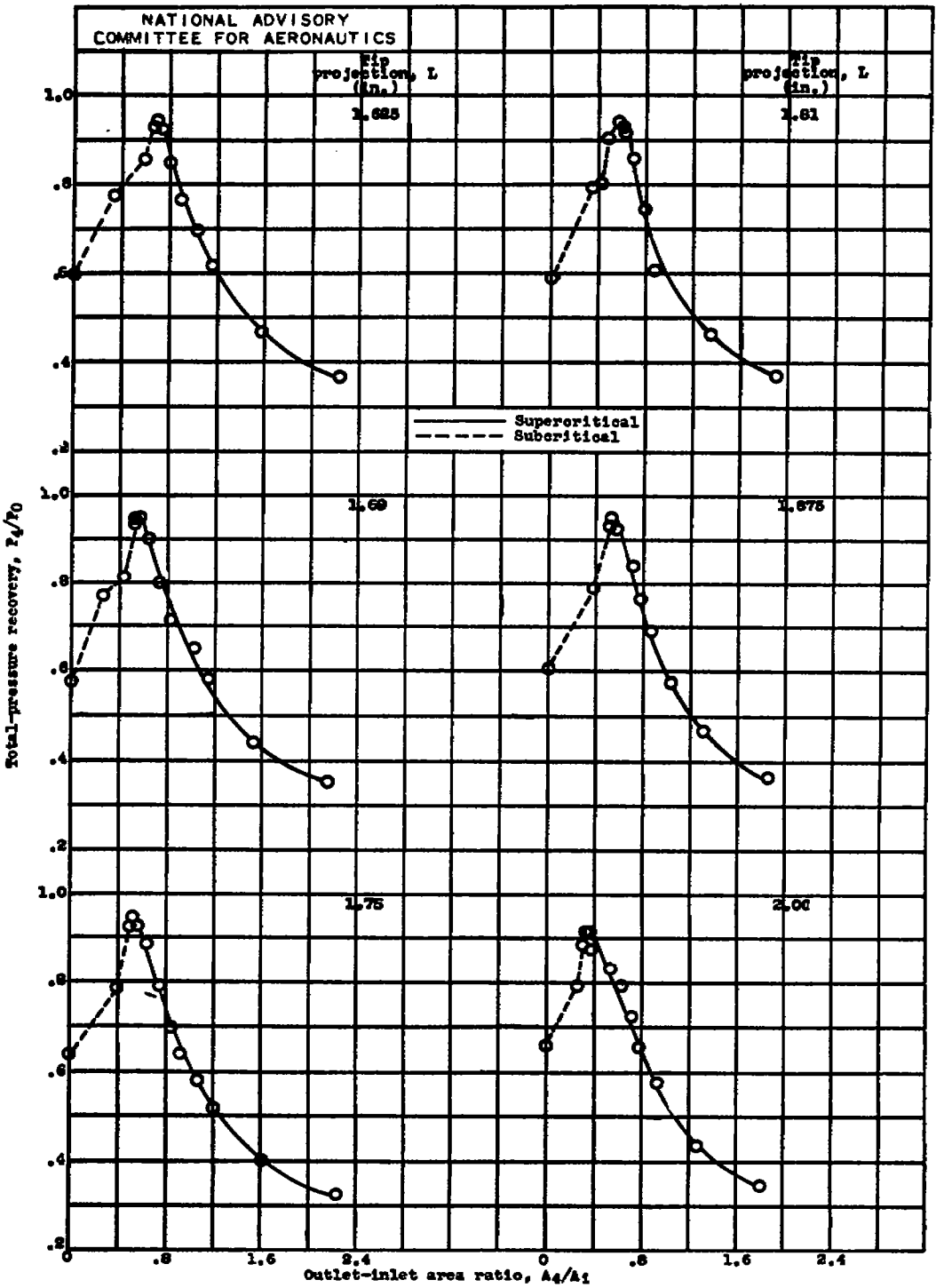

(c) Configuration B, parabolic-arc cone, curved inlet.

(d) Configuration B, parabolic-arc cone, straight inlet.

Figure 5.- Continued. Variation of total-pressure recovery with outlet-inlet area ratio at angle of attack of 0°.

[redacted]

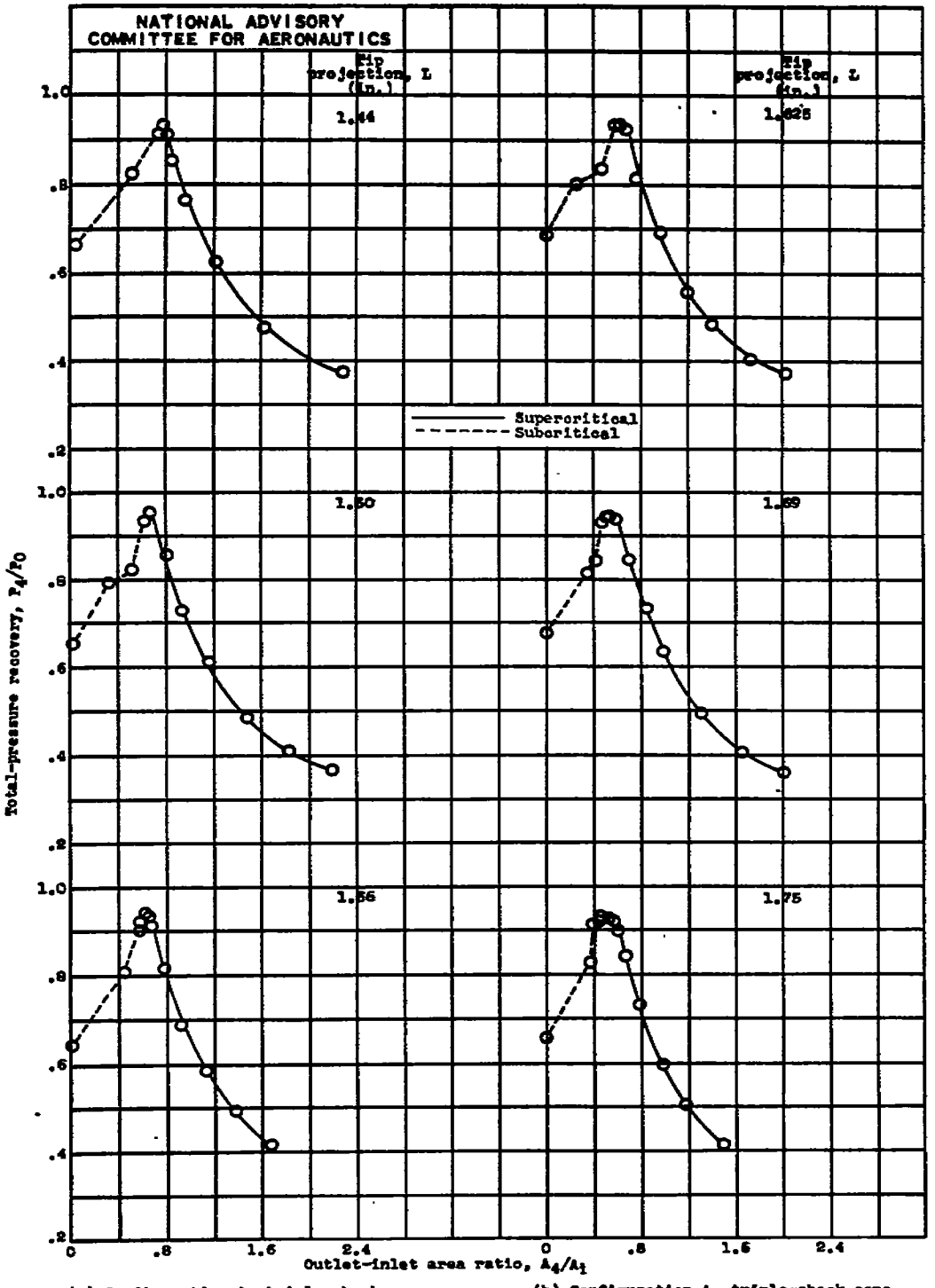

(a) Configuration A, triple-shock cone, curved inlet.

(b) Configuration A, triple-shock cone, straight inlet.

Figure 5.- Variation of total-pressure recovery with outlet-inlet area ratio at angle of attack of 0°.

[redacted]

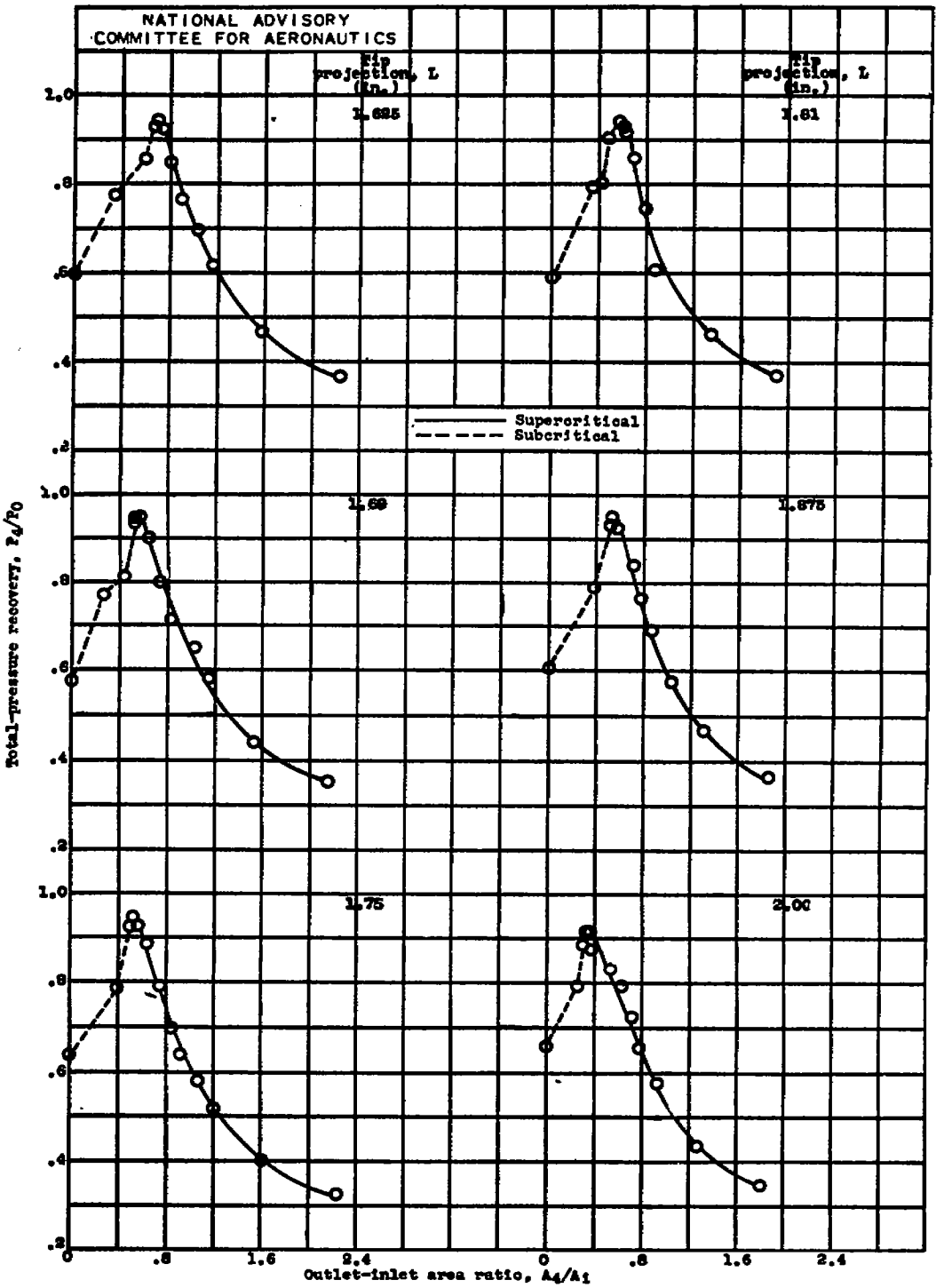

(c) Configuration B, parabolic-arc cone, curved inlet.

(d) Configuration B, parabolic-arc cone, straight inlet.

Figure 8.- Continued. Variation of total-pressure recovery with outlet-inlet area ratio at angle of attack of 0°.

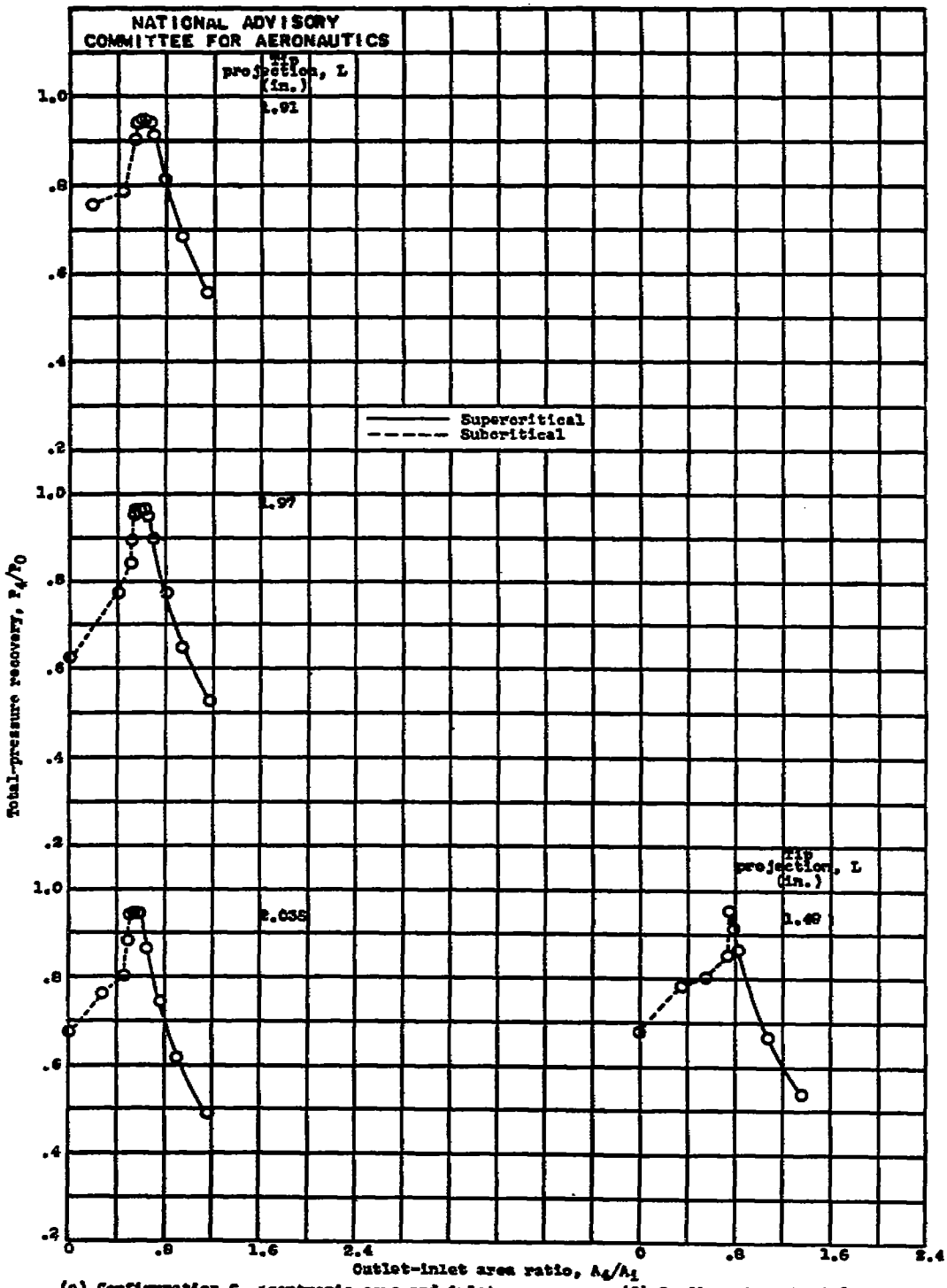

(e) Configuration C, isentropic cone and inlet.

(f) Configuration D, 30° cone and perforated straight inlet.

Figure 5.- Concluded. Variation of total-pressure recovery with outlet-inlet area ratio at angle of attack of 0°.

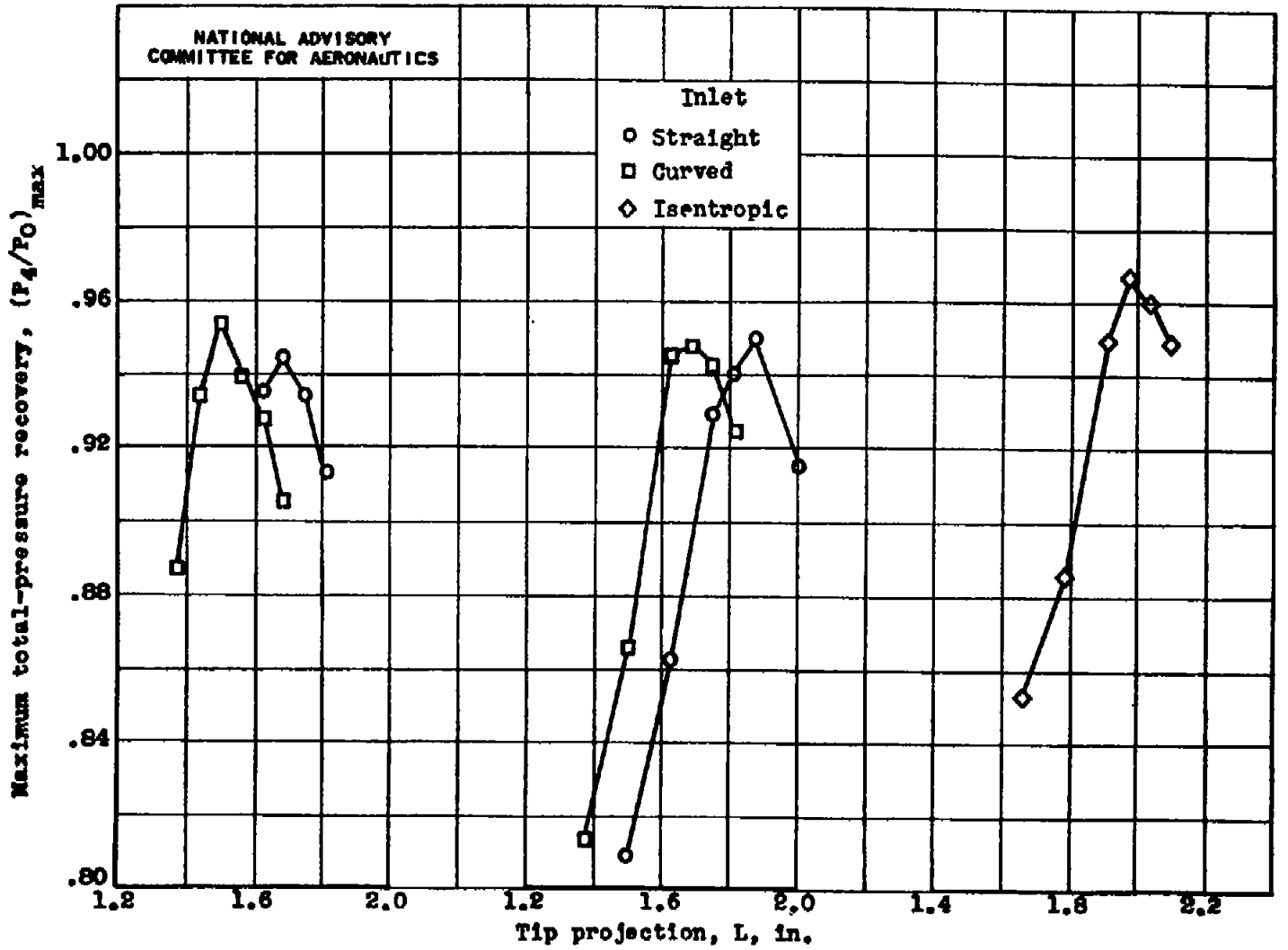

(a) Configuration A, triple-shock cone.

(b) Configuration B, parabolic-arc cone.

(c) Configuration C, isentropic cone and inlet.

Figure 6.- Variation of maximum total-pressure recovery with tip projection.

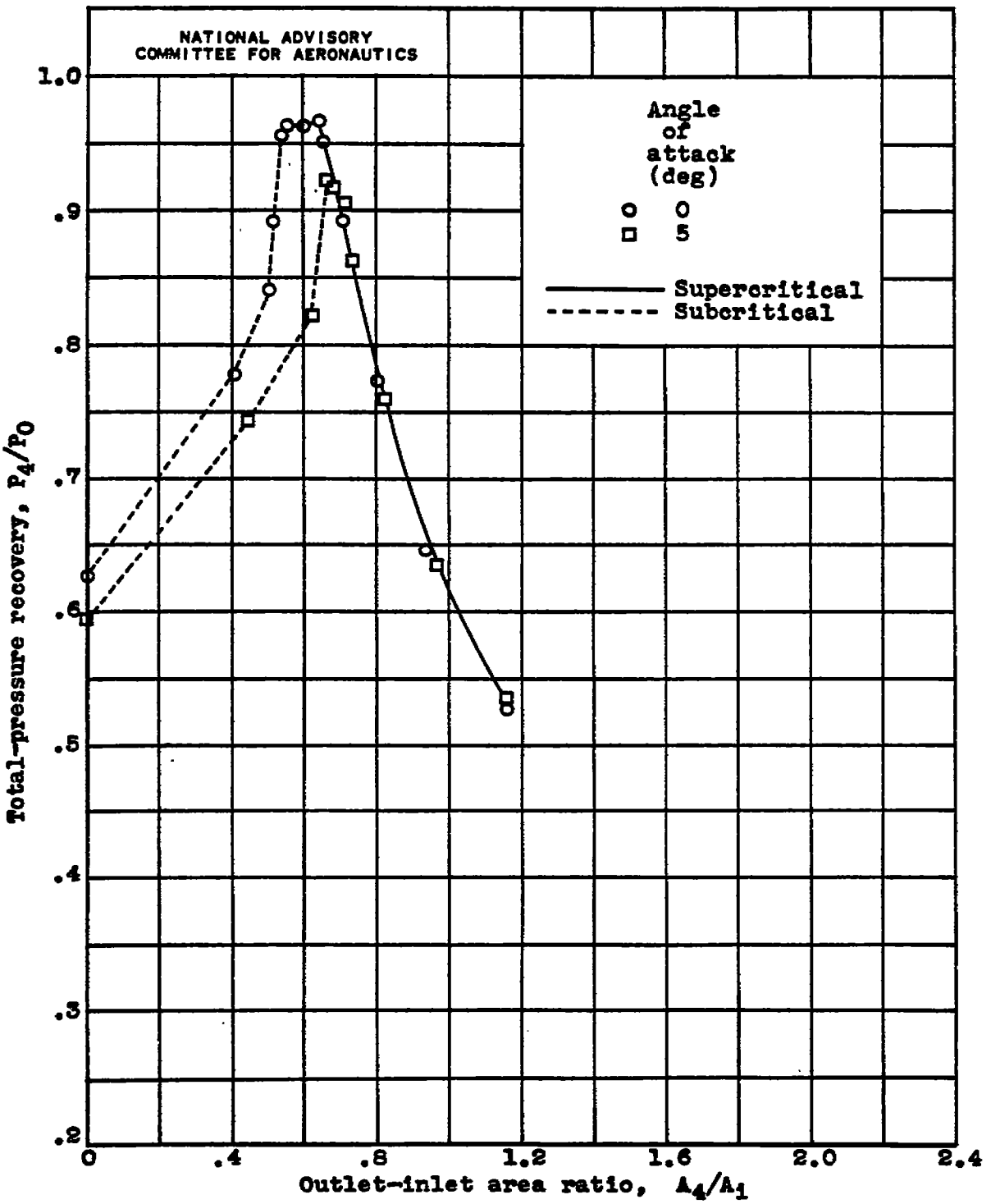

Figure 7.- Effect of angle of attack on pressure recovery obtained with isentropic cone at L = 1.97 inches.

[redacted]